



RK
LB-893

EXPERIMENTALLY DETERMINED

RADIATION CHARACTERISTICS OF

CONICAL AND TRIANGULAR ANTENNAS

RADIO CORPORATION OF AMERICA
RCA LABORATORIES DIVISION
INDUSTRY SERVICE LABORATORY

LB-893

1 OF 17 PAGES

OCTOBER 31, 1952

RADIO CORPORATION OF AMERICA
RCA LABORATORIES DIVISION
INDUSTRY SERVICE LABORATORY

LB-893

Experimentally Determined

Radiation Characteristics of Conical and Triangular Antennas

This report is the property of the Radio Corporation of America and is loaned for confidential use with the understanding that it will not be published in any manner, in whole or in part. The statements and data included herein are based upon information and measurements which we believe accurate and reliable. No responsibility is assumed for the application or interpretation of such statements or data or for any infringement of patent or other rights of third parties which may result from the use of circuits, systems and processes described or referred to herein or in any previous reports or bulletins or in any written or oral discussions supplementary thereto.

Approved



Experimentally Determined Radiation Characteristics of Conical and Triangular Antennas

Introduction

The usefulness of large-area radiators for broad-band applications has been amply demonstrated.¹ Antenna designers have utilized various geometrical shapes; cylindrical, conical, triangular and spheroidal.

Many articles have been published on the theoretical analysis of certain radiator shapes. In particular, the conical radiator has received considerable attention.²⁻⁸ The theoretical treatment involves simplifying assumptions and approximations in order to satisfy the required boundary conditions and to reduce the mathematical difficulties. Calculations following the analysis are indeed laborious. An alternative and easier approach to obtain a large amount of engineering data is that of direct experimental measurement.

Although some experimental results have been published by Essen and Oliver,⁹ the extent of their coverage is limited.

The data described in this bulletin were obtained during 1945 from experimental impedance and radiation measurements on two types of broad-band radiators, conical and triangular antennas. These particular shapes were chosen for their simplicity of construction as well as for the ease in applying the data to practical feed systems. This work was carried on as a logical step following previously made impedance measurements on cylindrical antennas.¹⁰

Useful design information was obtained experimentally on the radiation characteristics of conical and triangular antennas for wide variations in their physical dimensions. The data are presented graphically in terms of the input resistance and reactance, field patterns, and relative power gain. A comparison of the measured values for conical antennas is made with a small number of published theoretical values, with excellent agreement.

Method of Measurement

The impedance data were obtained with the use of a conventional slotted transmission line and sliding probe. The probe led to an accurately calibrated superheterodyne receiver which indicated the voltage standing-wave ratio on the line as well as the position of the voltage minimum. From this information the antenna impedance was calculated by the use of transmission-line charts.

Most of the data were secured using a frequency of 500 Mc. This choice of frequency, having a wavelength of approximately two feet, permits the easy manipulation of most of the antenna models, and yet is not too high to affect the accuracy of the measurements. A few of the very largest cones and triangles, however, were measured at a frequency of 1670 Mc to facilitate handling the antennas.

In order to provide a minimum-length transmission line to the slotted measuring line and also furnish shielding of the measuring apparatus and operator, only one half of the test dipole was fed against a large image or ground plane (see Fig. 1). Hence all measured impedance values plotted are one-half the values that would be obtained from a balanced dipole.

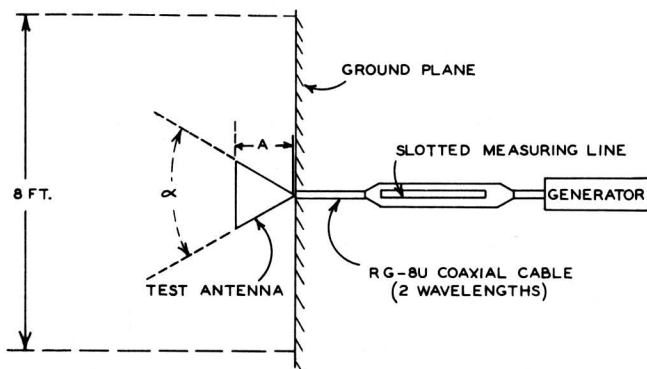


Fig. 1 - Arrangement of apparatus in making the impedance measurements.

The ground plane consisted of a conductive disk eight feet in diameter. This size is sufficiently large (approximately four wavelengths) so that the impedance errors due to the use of a finite plane instead of an infinite plane are of second-order effect.

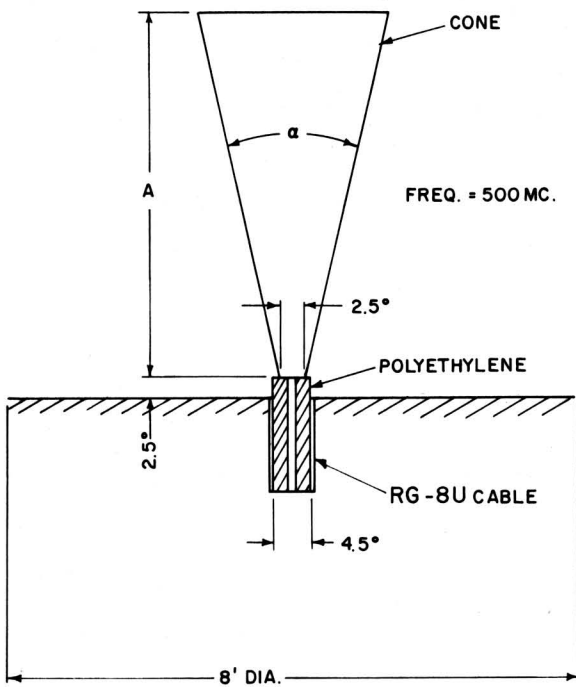


Fig. 2 - Enlarged view of the unipole feed.

The setup was supported in the clear on high trestles to reduce the effect of the earth, buildings, etc., to a minimum.

Fig. 2 shows an enlarged view of the unipole feed details. In order to provide a good mechanical means of attachment to the inner conductor of the feed line, the test unipole point was cut off to furnish a truncated mounting base of 2.5 electrical degrees in width. The polyethylene insulation of the RG-8U coaxial cable was extended 2.5 electrical degrees beyond the ground screen as shown. All dimensions in electrical degrees are obtained from the product of the physical dimension and the ratio, $360/\text{wavelength}$. The wavelength and the physical dimensions are measured in the same units.

All impedances are referred to the junction of the coaxial line and the ground plane. Corrections were made on high standing-wave ratios to compensate for the slight loss in the RG-8U feed cable joining the test antenna and the slotted measuring line.

The flare angle of the cones and triangles is designated by the angle, α , in degrees. The length, A , of the antenna in electrical degrees is measured from the top to the truncated base.

For the larger test antennas the free end was supported from above by a small polyethylene insulator and long waxed string.

Both the conical and triangular antennas were constructed of copper-plated sheet steel having a thickness of 0.020 inch. The large ends of the cones were not closed. For a given test antenna, measurements were made as the length was cut down.

Field patterns were taken on balanced conical dipoles as shown in Fig. 3. The conical dipole was supported with its longitudinal axis horizontal above a motor-driven turntable. A coaxial line from the generator led through the vertical support pipe to a balun, which insures a balanced feed, to the test antenna. Long polystyrene rods supported the free ends of the larger dipoles.

The output of a directive receiving antenna located approximately 150 feet away led to a superheterodyne receiver. The receiver output operated an Esterline-Angus recorder.

As the conical dipoles have circular symmetry in the vertical plane, only one field pattern was taken on each test antenna.

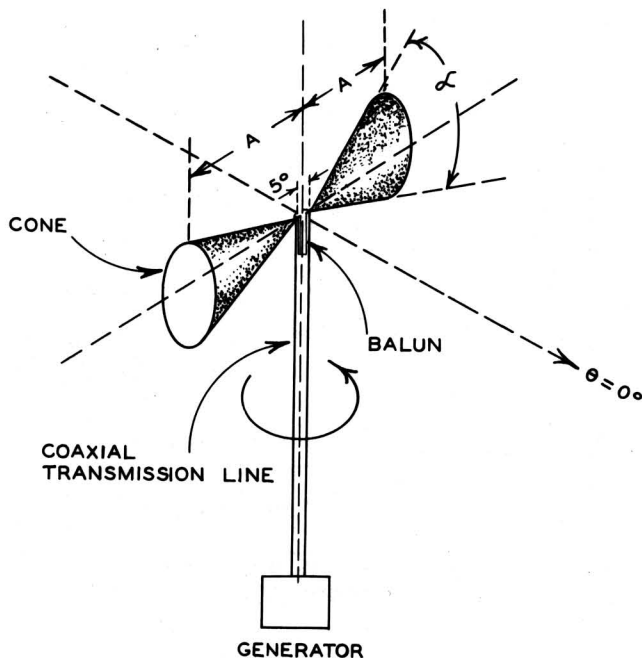


Fig. 3 - Arrangement of apparatus in making field pattern measurements.

Since the flat triangular dipoles do not have such symmetry in the vertical plane, three measurements are necessary to obtain sufficient information on the space radiation.

Referring to Fig. 4, field patterns were measured on the triangular dipoles in the XY plane as with the conical dipoles. In addition, field patterns were taken in the XZ plane. The

latter was accomplished simply by rotating the triangular dipole 90 degrees on its longitudinal axis and repeating the pattern measurement.

As the only points common to these two patterns lie on the X axis where the radiation is zero, one other measurement is required to ascertain the relative amplitudes of the two patterns. In order to eliminate any possible ground reflection error, this information was obtained using the impedance measuring setup of Fig. 1. The ground plane was mounted horizontally with one-half of the test triangle extending vertically above. A vertical receiving antenna with high directivity was placed a great distance away with its center lying in the plane of the ground plane. Hence, currents flowing in the ground plane produce canceling fields at the receiving antenna, and reception is obtained only from the vertical test antenna.

Relative field strength measurements were taken for two positions of the triangular unipole; one with the vertical receiving antenna lying in the plane of the triangle, and the other with the triangle rotated 90 degrees on its vertical axis.

These data, giving the relative field strengths along the Y and Z axes, respectively, supplied the necessary information to correlate the two field patterns taken in the XY and XZ planes.

Conical Antenna Impedance Measurements

The measured impedance data taken on the conical unipoles are plotted vs the radiator length in Figs. 5 and 6 in terms of the resistance and reactance values. Curves are given for various flare angles up to a value of $\alpha = 90$ degrees. The limiting case of $\alpha = 0$ degrees represents a cylindrical radiator having a diameter of 2.5 electrical degrees since the feed point was kept fixed at that diameter.

As the flare angle increases, the amplitude of the resistance and reactance variations decreases. It is seen, for example, that a 90-degree conical unipole has a resistance of approximately 50 ohms and very low reactance over a very wide frequency range.

The resistance peaks in Fig. 5 are re-plotted in Fig. 7 to show the maximum resistance

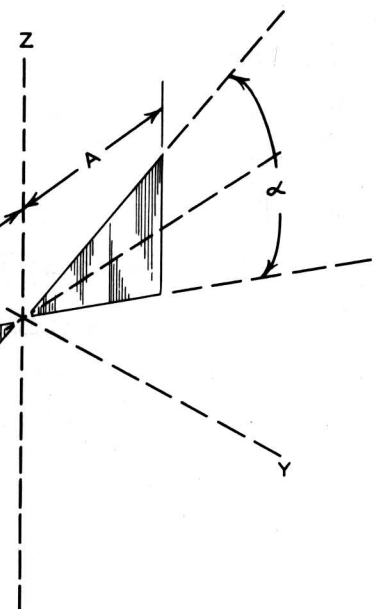


Fig. 4 - Geometry of the triangular dipole.

Experimentally Determined Radiation Characteristics of Conical and Triangular Antennas

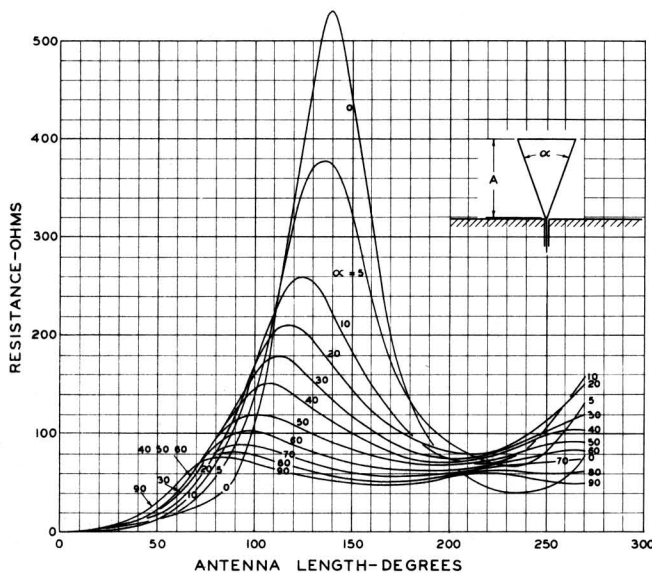


Fig. 5 - Measured resistance curves of the conical unipole vs length in electrical degrees for various flare angles.

variation vs the flare angle. Also given in Fig. 7 is the radiator length for maximum resistance. These points correspond quite closely to the second resonance values.

Fig. 8 shows the antenna lengths for the first resonance plotted against the flare angle.

Some question has arisen in the past as to the effect of closing the open end of the cone with a plane conducting cover. Time did not permit repeating all measurements with closed ends. However, the impedance of a cone having a

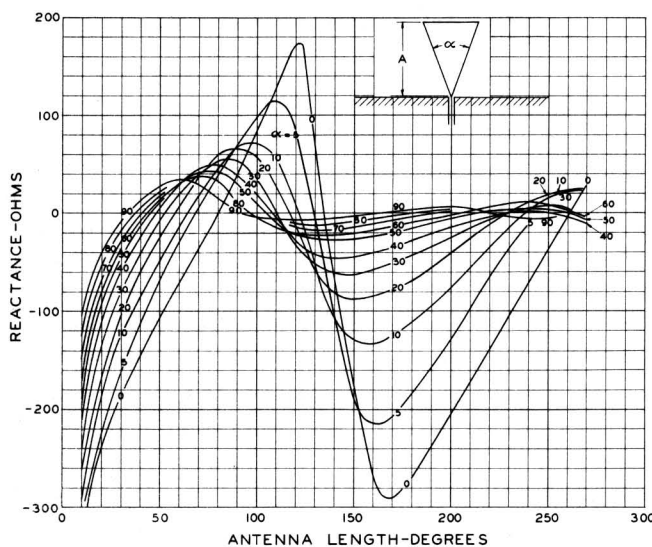


Fig. 6 - Measured reactance curves of the conical unipole vs length in electrical degrees for various flare angles.

flare angle of 60 degrees was determined with its end closed for various lengths. No measurable differences in impedance were detected.

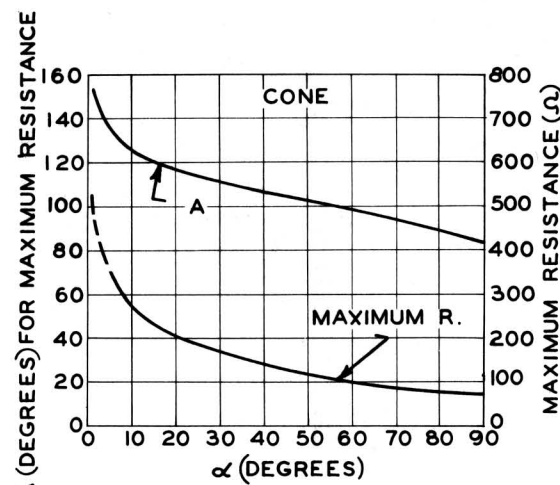


Fig. 7 - Maximum conical unipole resistance vs the flare angle in degrees, and the unipole length in electrical degrees at which the maximum resistance occurs vs the flare angle.

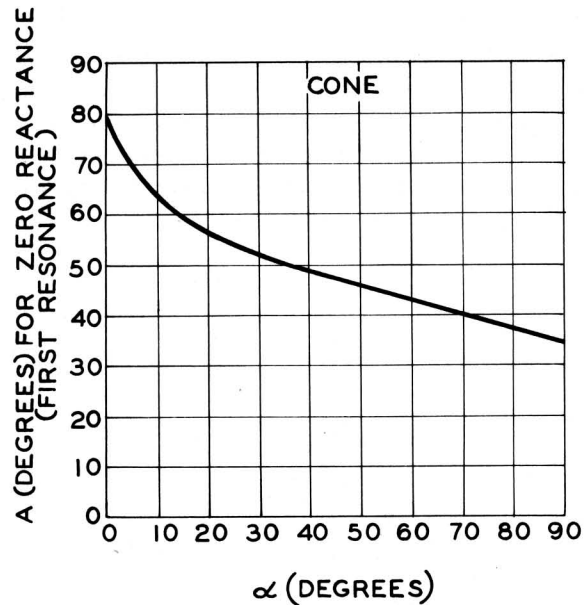


Fig. 8 - The conical unipole length in electrical degrees for zero reactance vs the flare angle.

An interesting comparison is given in Figs. 9 and 10 between the measured data given here and the calculated values presented by Papas and King⁸ for a 60-degree flare-angle cone. The cone assumed by Papas and King was capped with a spherical section, while that herein described was open-ended. Fig. 9 shows

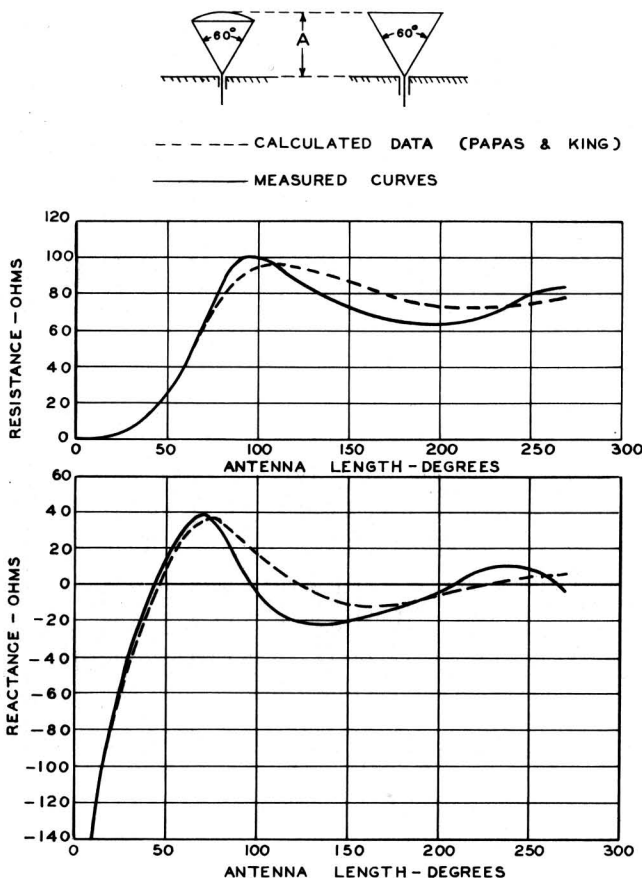


Fig. 9 - Comparison of calculated and measured impedance curves for a 60° flare-angle conical unipole.

the comparative results where A is the overall length of the cone and cap in the theoretical case while A is the length of the uncapped cone in the measured case. A substantial agreement between the theoretical and experimental values may be noted.

In Fig. 10, the data of Fig. 9 are displayed so that A is the length of the cone proper in both the case of the theoretical values and the measured data. An even greater correlation is seen.

Conical Antenna Field Pattern Measurements

For each value of flare angle, field patterns were measured for half-lengths (A) from 60 to 180 electrical degrees in 30-degree steps, and from 180 to 270 electrical degrees in 15-degree steps. Closer intervals of measurement were taken for the longer antennas as

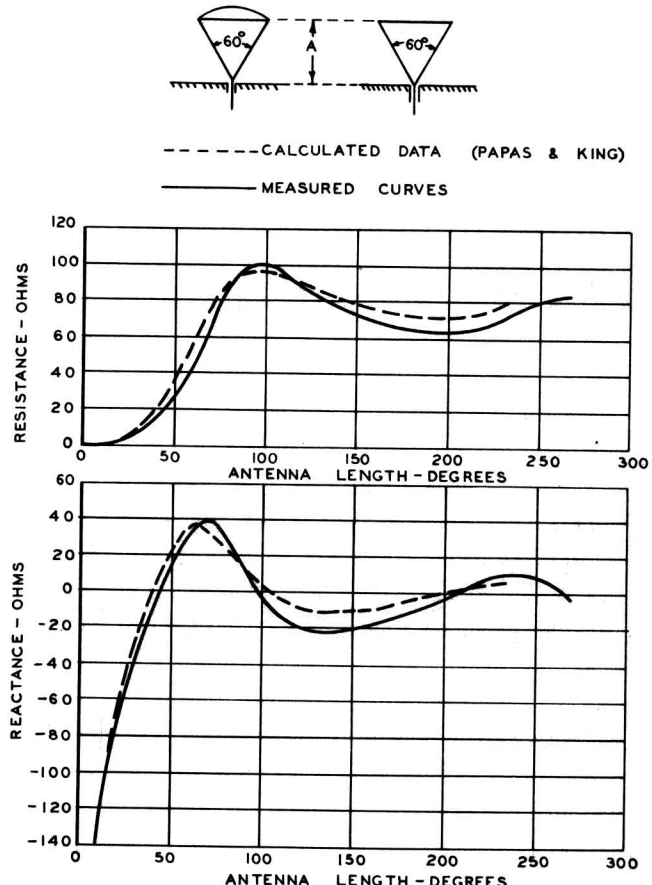


Fig. 10 - Comparison of calculated and measured impedance curves for a 60° flare-angle conical unipole.

the field configurations change more rapidly in that region.

Since the patterns are symmetrical about the major axes, only one quadrant is given (Figs. 11 to 22). The patterns are plotted in rectangular coordinates, showing the relative field strength vs azimuth angle. Also included for comparison are the field patterns (Fig. 11) for a thin wire calculated on the basis of sine-wave distribution.

It is seen that the sharp nulls of the longer conical dipoles are gradually filled in as the flare angle is increased to approximately 50 degrees. For larger flare angles, the secondary lobes commence to become prominent again.

For lengths less than 180 electrical degrees, no side lobes appear for any of the measured flare angles.

Field patterns were also repeated on a 60-degree flare-angle conical dipole with closed ends. The patterns were practically

Experimentally Determined Radiation Characteristics of Conical and Triangular Antennas

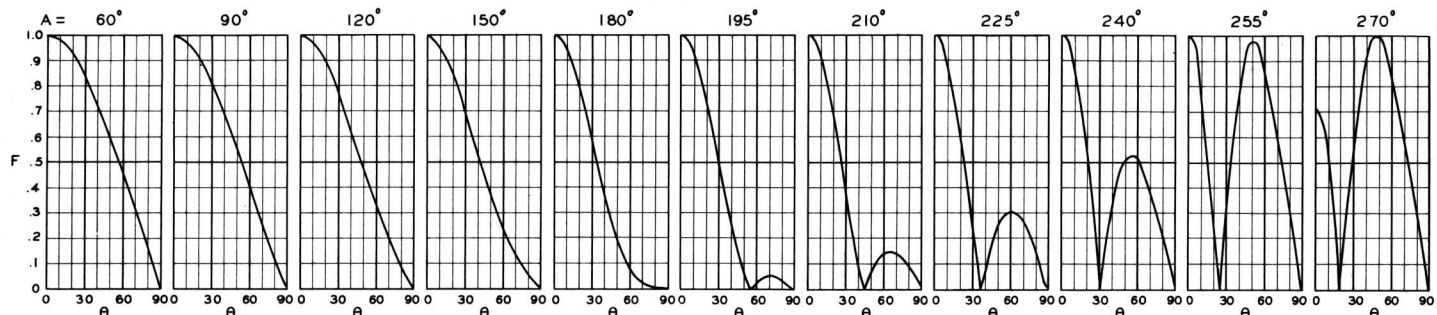


Fig. 11 - Calculated field patterns of a thin-wire (theoretical) dipole.

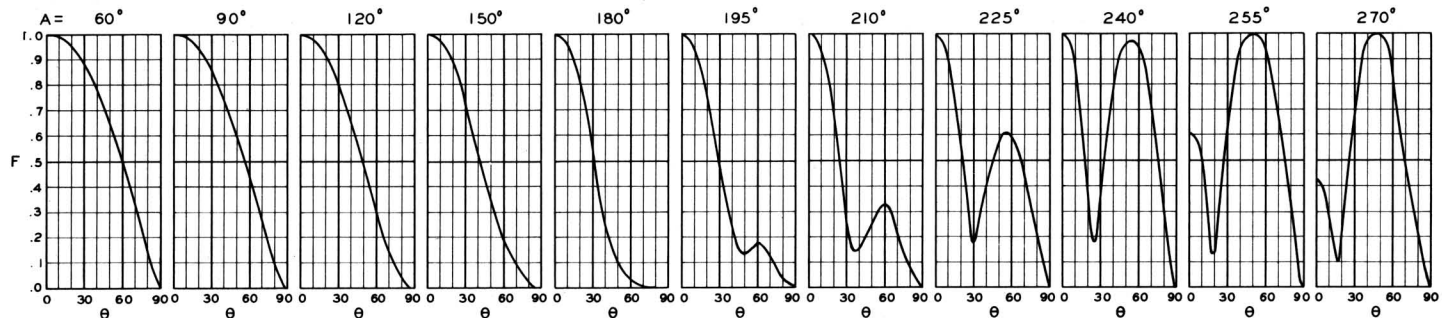


Fig. 12 - Measured field patterns of a conical dipole for various dipole lengths and flare angle (α) = 0° .

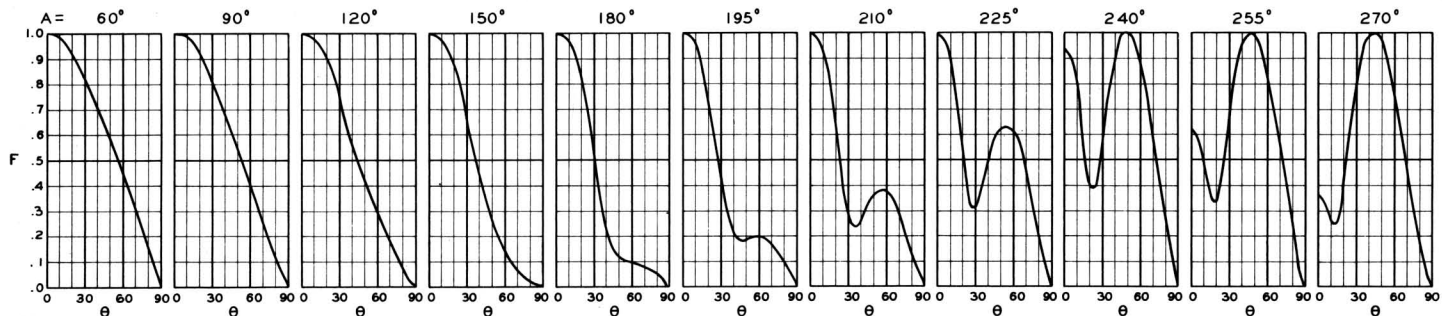


Fig. 13 - Measured field patterns of a conical dipole for various dipole lengths and flare angle (α) = 5° .

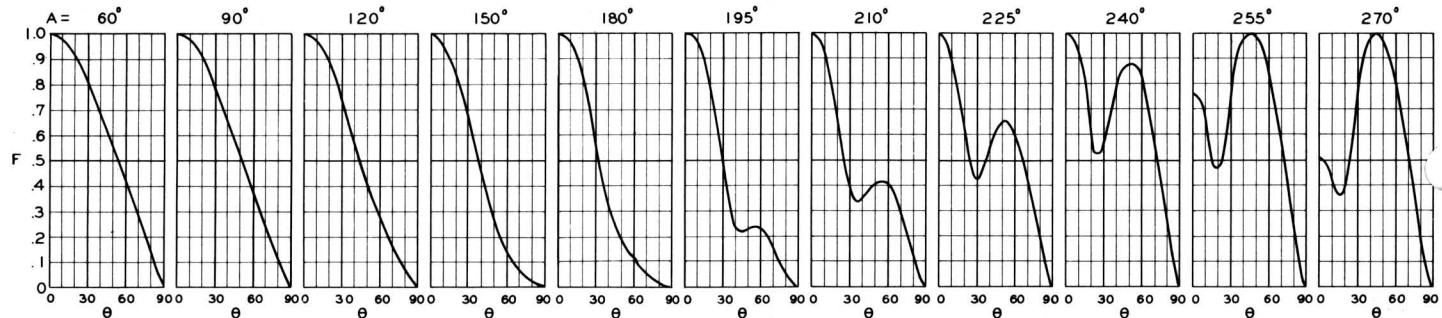


Fig. 14 - Measured field patterns of a conical dipole for various dipole lengths and flare angle (α) = 10° .

Experimentally Determined Radiation Characteristics of Conical and Triangular Antennas

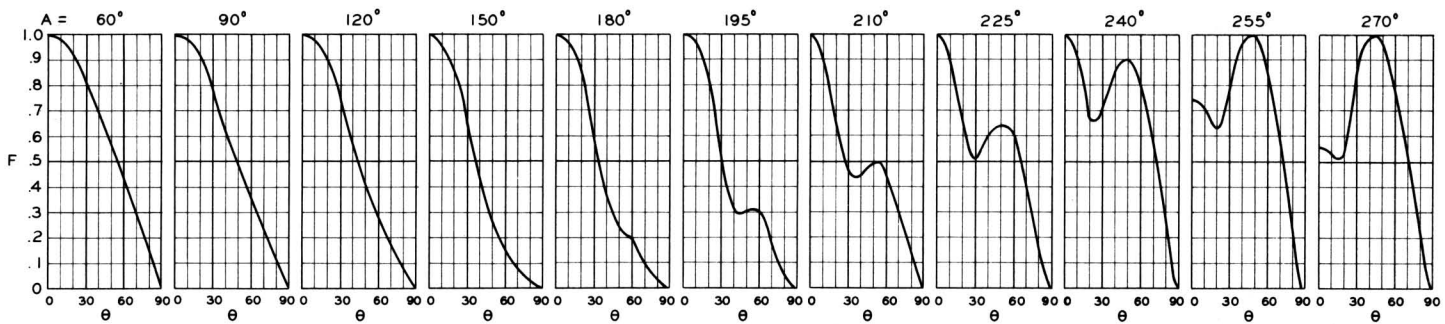


Fig. 15 - Measured field patterns of a conical dipole for various dipole lengths and flare angle (α) = 20° .

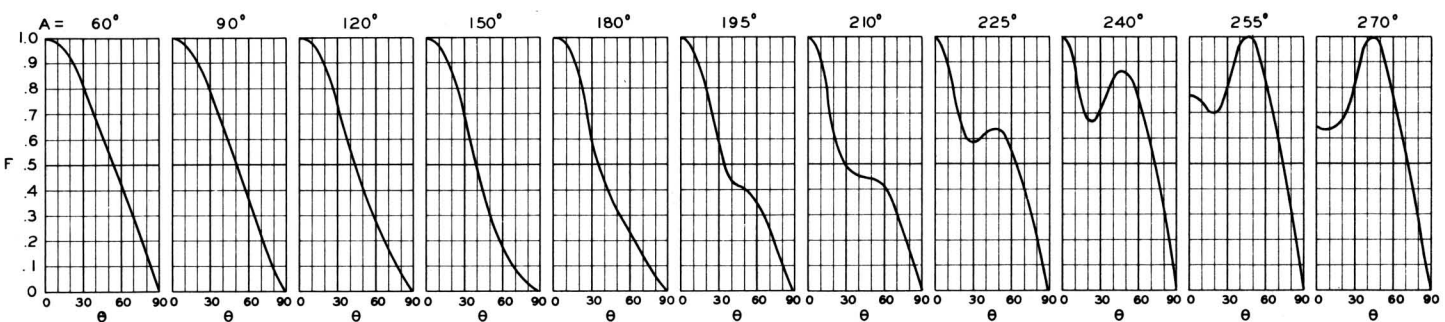


Fig. 16 - Measured field patterns of a conical dipole for various dipole lengths and flare angle (α) = 30° .

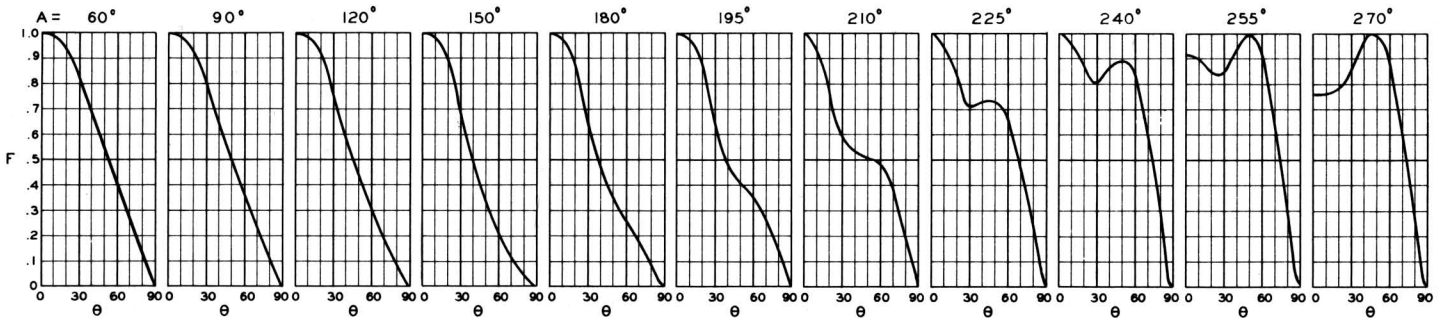


Fig. 17 - Measured field patterns of a conical dipole for various dipole lengths and flare angle (α) = 40° .

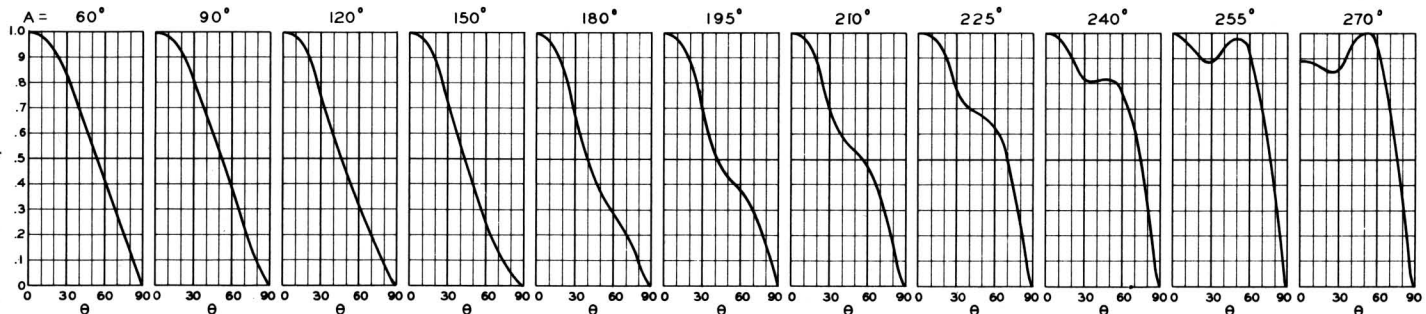


Fig. 18 - Measured field patterns of a conical dipole for various dipole lengths and flare angle (α) = 50° .

Experimentally Determined Radiation Characteristics of Conical and Triangular Antennas

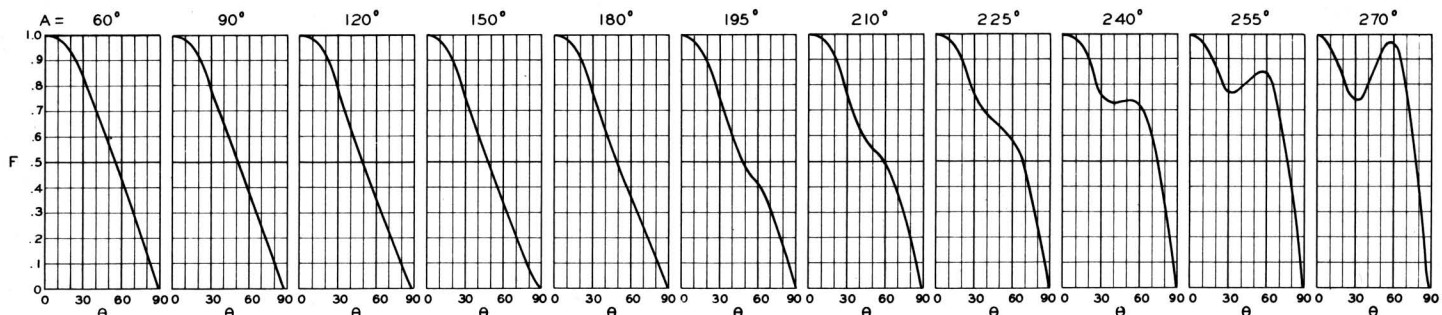


Fig. 19 - Measured field patterns of a conical dipole for various dipole lengths and flare angle (α) = 60° .

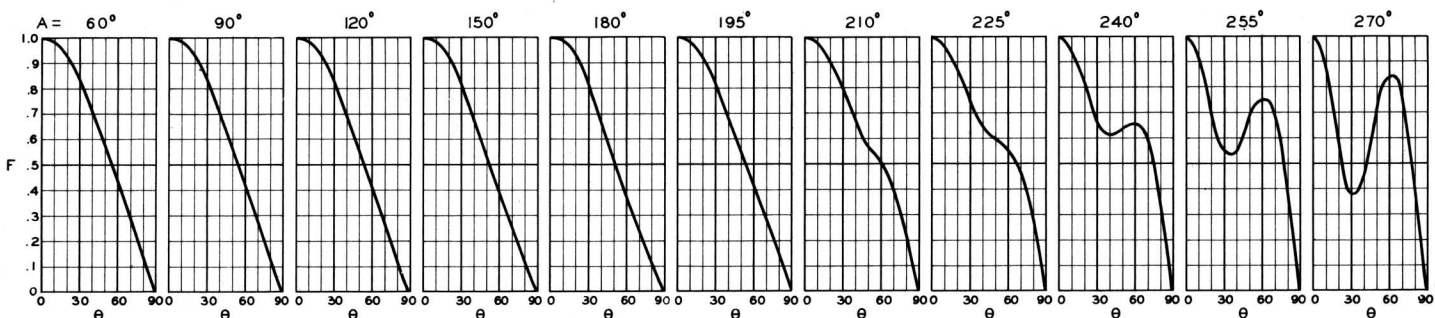


Fig. 20 - Measured field patterns of a conical dipole for various dipole lengths and flare angle (α) = 70° .

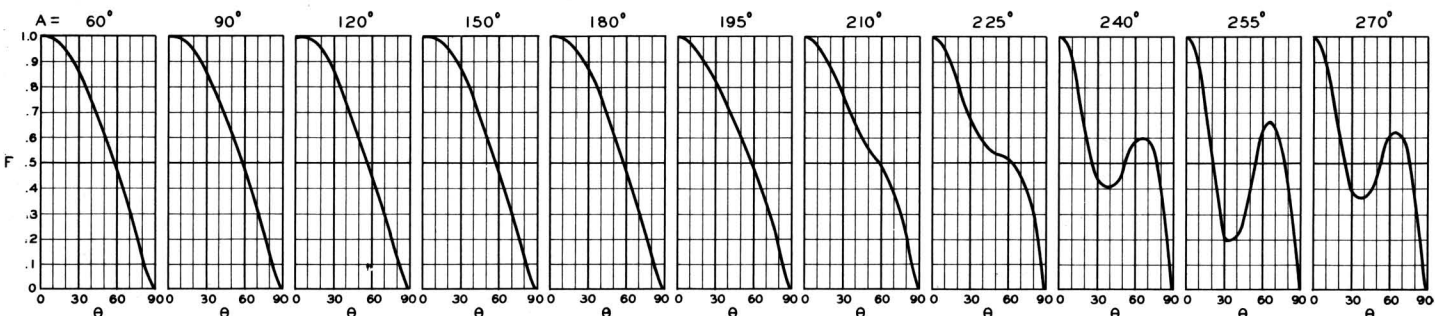


Fig. 21 - Measured field patterns of a conical dipole for various dipole lengths and flare angle (α) = 80° .

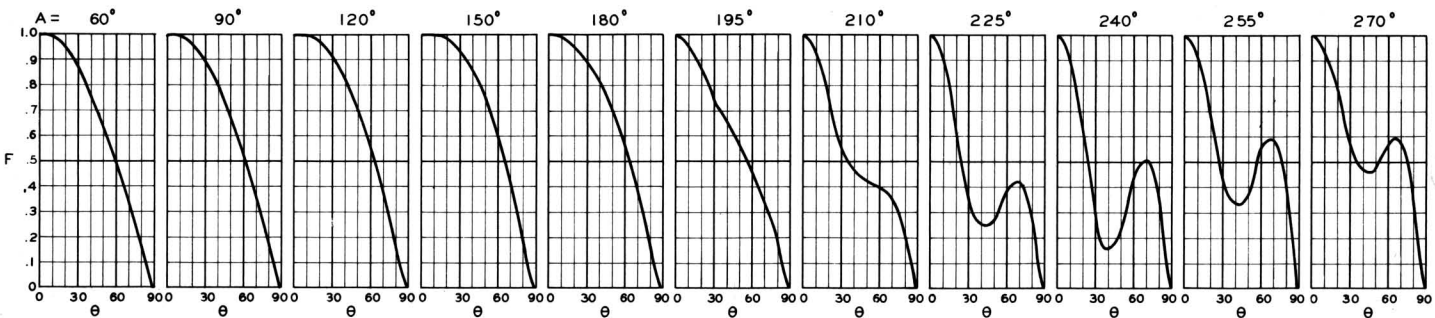


Fig. 22 - Measured field patterns of a conical dipole for various dipole lengths and flare angle (α) = 90° .

Experimentally Determined Radiation Characteristics of Conical and Triangular Antennas

identical with those obtained with the ends open.

Calculations by Papas and King⁷ on the radiation characteristics of a 60-degree flare-angle cone for three different antenna lengths are compared with the measured data in Fig. 23. A close agreement is observed, when the comparison is made on the basis of the overall height of the capped cone in the theoretical case with the height of the uncapped cone in the measured instance.

This leads to the postulate that the addition of the spherical cap effectively lengthens the cone by an amount which is the radius of the spherical cap minus the height of the cone, with respect to the radiation patterns, while the addition of the spherical cap does not affect the impedance.

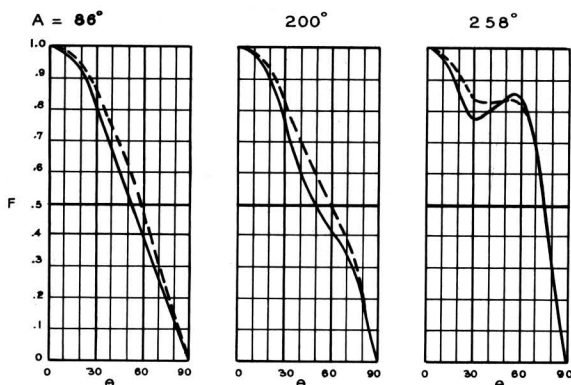
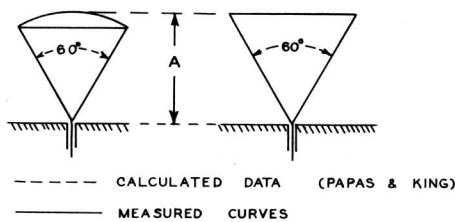


Fig. 23 - Comparison of calculated and measured radiation characteristics of a 60° flare-angle conical dipole.

Conical Antenna Power Gain Calculations

The uniform radiation in the plane normal to the axis of the conical dipoles facilitates the power gain calculations. The radiated energy is an integrated function of the square of the distant field strength times the cosine of the

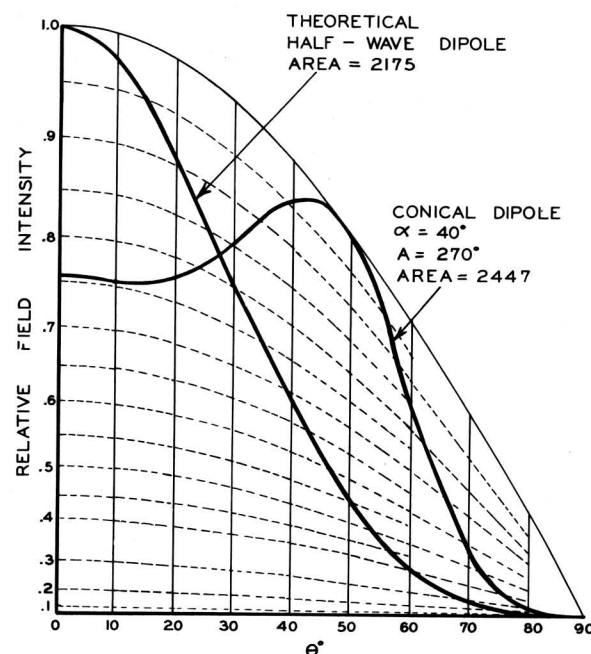


Fig. 24 - An example of the relative power gain calculation for a 40° flare-angle conical dipole.

azimuth angle, θ . The measured conical field patterns are replotted on a form shown in Fig. 24, in which the coordinates are $F_o^2 \cos \theta$ and θ . Hence the relative power integration is mechanically performed by planimetering the area enclosed by the replotted curve. The area under the theoretical field pattern of a half-wave dipole is also measured as a reference. The ratio of the two areas is then the relative maximum power gain of the conical dipole with respect to a theoretical half-wave dipole.

In the example given in Fig. 24, the patterns of a 270-degree conical dipole having

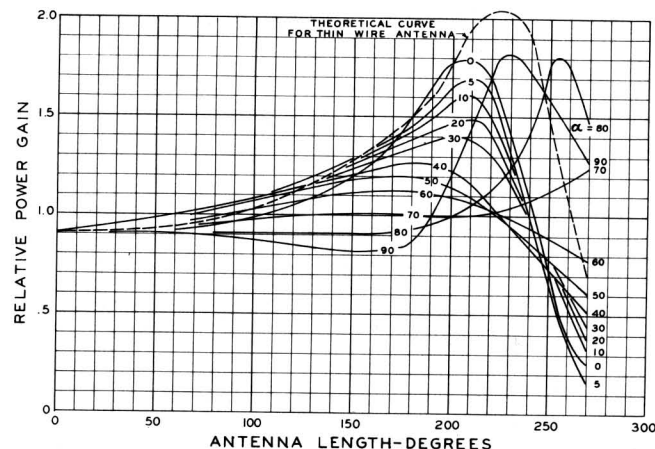


Fig. 25 - Calculated power gain curves of the conical dipoles with respect to a theoretical half-wave dipole.

Experimentally Determined Radiation Characteristics of Conical and Triangular Antennas

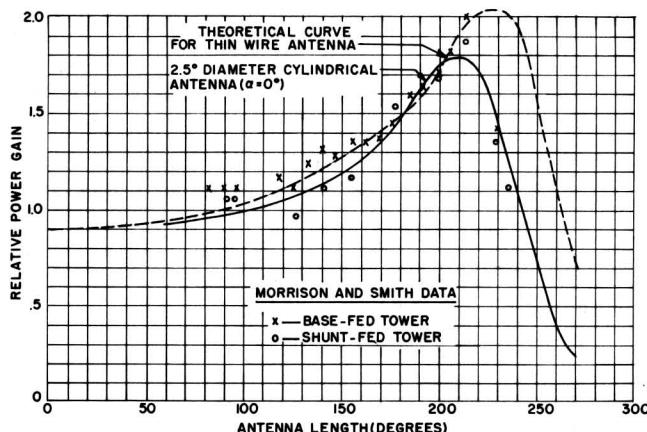


Fig. 26 - Comparison of calculated and measured power-gain data.

a flare angle of 40 degrees and a theoretical half-wave dipole are plotted. The maximum relative power gain is the ratio of the planimetered areas enclosed by the two curves, or

$$P.G._{MAX} = \frac{2175}{2444} = 0.89$$

As the relative field intensity is 0.76 at zero azimuth angle for the conical dipole, the relative power gain for this broad-side condition is the maximum power gain reduced by the square of the relative field intensity, or

$$P.G.(\theta=0^\circ) = 0.89 \times 0.76^2 = 0.514$$

The relative power gain curves at $\theta = 0^\circ$ computed in this manner for all of the measured

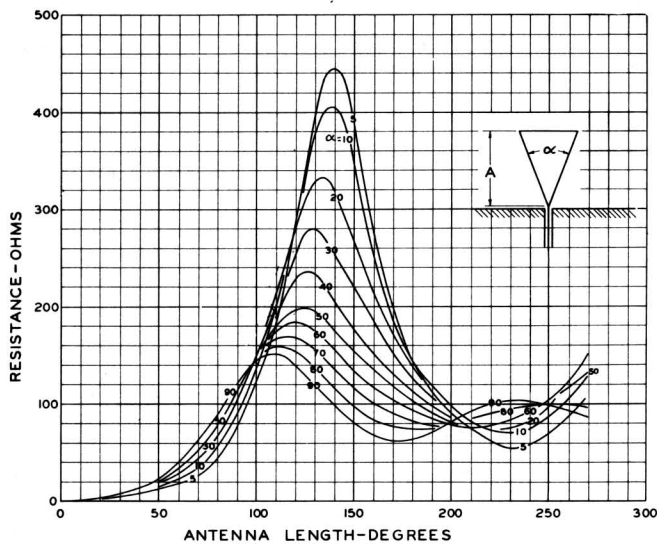


Fig. 27 - Measured resistance curves of the triangular unipole vs length in electrical degrees for various flare angles.

conical dipoles are given in Fig. 25. The different field pattern shapes of the thin-wire dipole (Fig. 11) and the cylindrical dipole (Fig. 12) result in a considerable departure in power gain for the longer antennas.

An experimental verification that the high power gains for long antennas shown by the theoretical curve of Fig. 25 are not realized with practical installations is given in Fig. 26. The relative power gains calculated from measured field strength data by Morrison and Smith¹¹ on a 400-foot broadcast tower are plotted for two types of tower excitation, base-fed being shown by the crosses and shunt-fed by the circles. The tower diameter was approximately 1½ electrical degrees for the quarter-wave length. It is seen that the Morrison and Smith data conforms much closer to the 2.5-degree diameter antenna than to the theoretical curve.

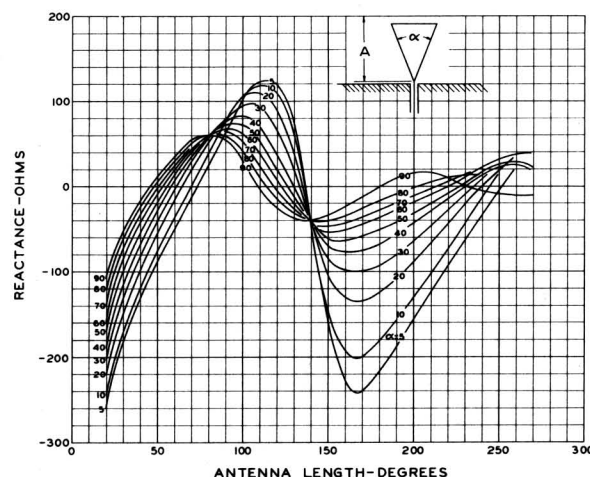


Fig. 28 - Measured reactance curves of the triangular unipole vs length in electrical degrees for various flare angles.

Triangular Antenna Impedance Measurements

The measured impedance data taken on the triangular unipoles are plotted in Figs. 27 and 28. In general, it is seen that the resistance and reactance fluctuations are greater than with the conical antennas for the same flare angle.

An interesting point may be noted (Fig. 28) in that for a length of 140 electrical degrees the reactance is independent of the flare angle of the triangle.

Experimentally Determined Radiation Characteristics of Conical and Triangular Antennas

The maximum resistance values and corresponding antenna lengths are shown in Fig. 29. A comparison of Figs. 7 and 29 show that for a given flare angle the cone peak resistance is

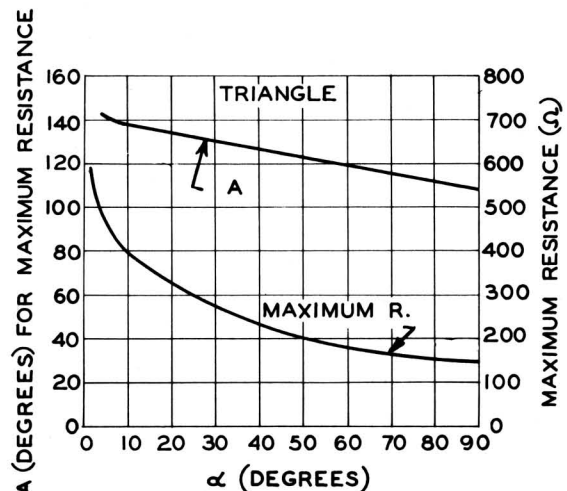


Fig. 29 - Maximum triangular unipole resistance vs the flare angle in degrees, and the unipole length in electrical degrees at which the maximum resistance occurs vs the flare angle.

considerably lower than the triangle peak resistance.

Fig. 30 shows the antenna length for the first resonance plotted vs the flare angle.

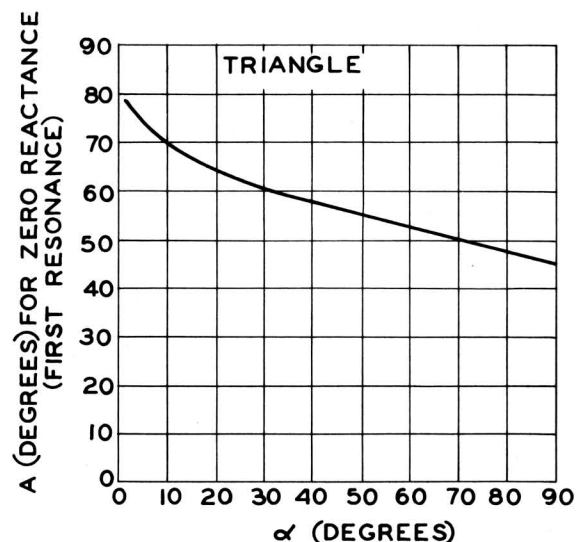


Fig. 30 - The triangular unipole length in electrical degrees for zero reactance vs the flare angle.

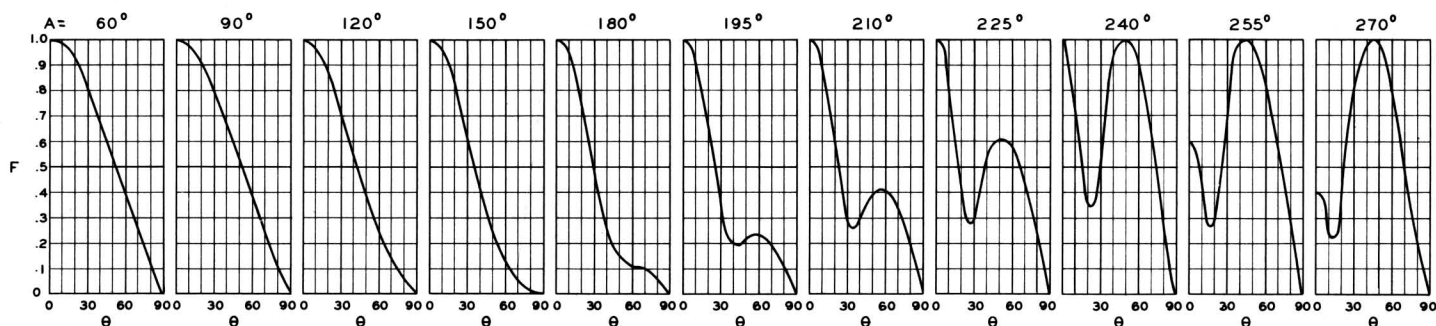


Fig. 31 - Measured field patterns of a triangular dipole for various dipole lengths and flare angle (α) = 5° . The patterns in the XZ plane are indicated by solid curves.

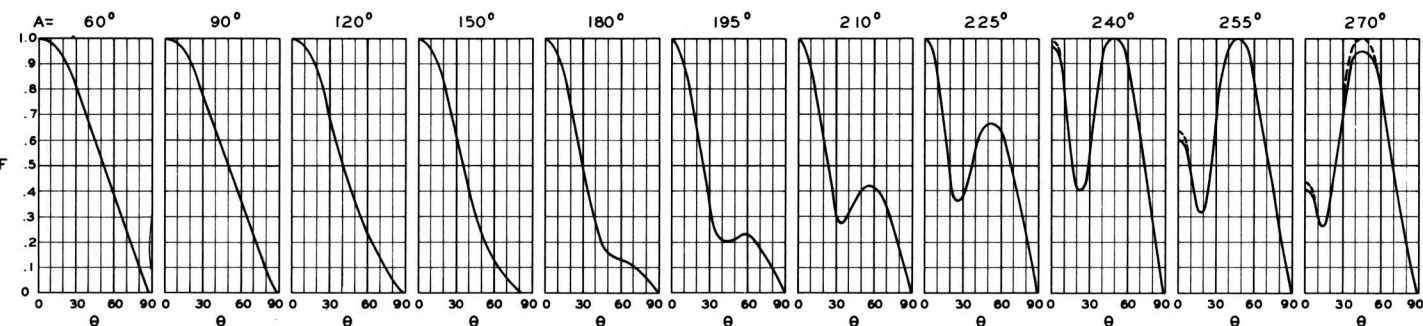


Fig. 32 - Measured field patterns of a triangular dipole for various dipole lengths and flare angle (α) = 10° . The patterns in the XZ plane are indicated by the solid curves, and the patterns in the XY plane by the dashed curves.

Experimentally Determined Radiation Characteristics of Conical and Triangular Antennas

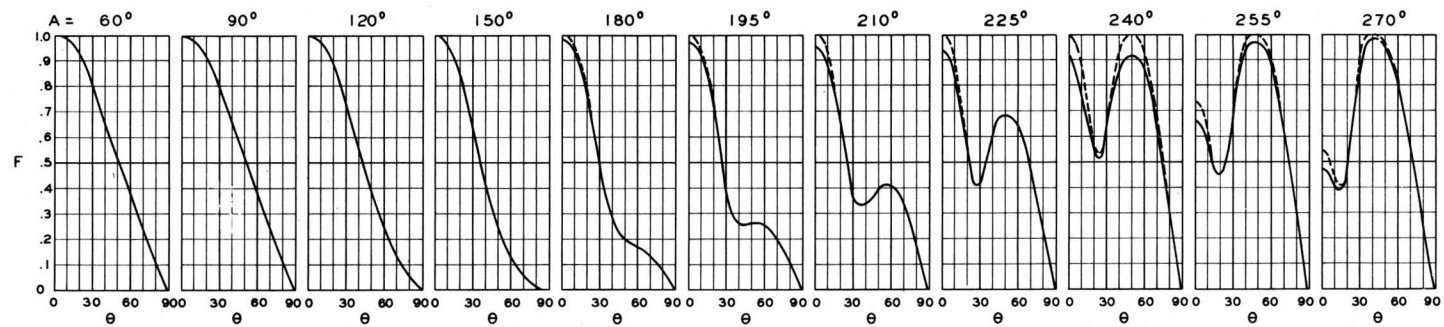


Fig. 33 – Measured field patterns of a triangular dipole for various dipole lengths and flare angle (α) = 20° . The patterns in the XZ plane are indicated by the solid curves, and the patterns in the XY plane by the dashed curves.

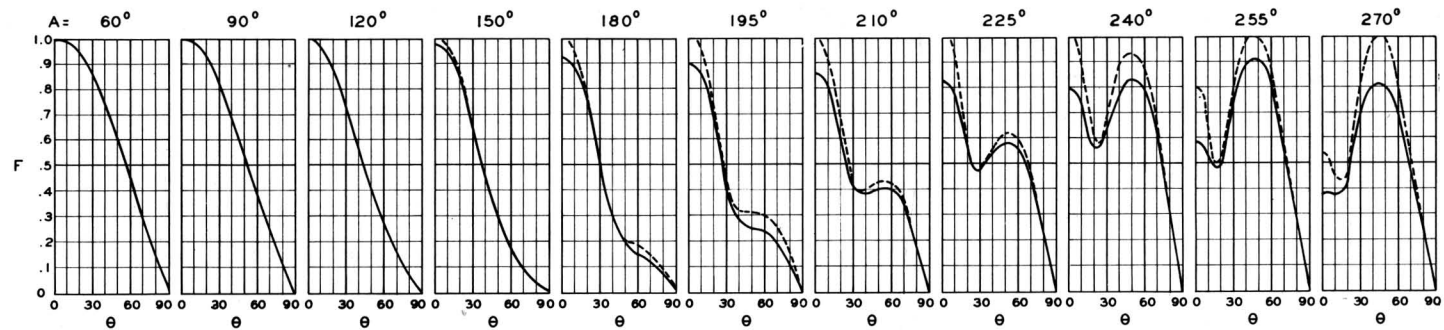


Fig. 34 – Measured field patterns of a triangular dipole for various dipole lengths and flare angle (α) = 30° . The patterns in the XZ plane are indicated by the solid curves, and the patterns in the XY plane by the dashed curves.

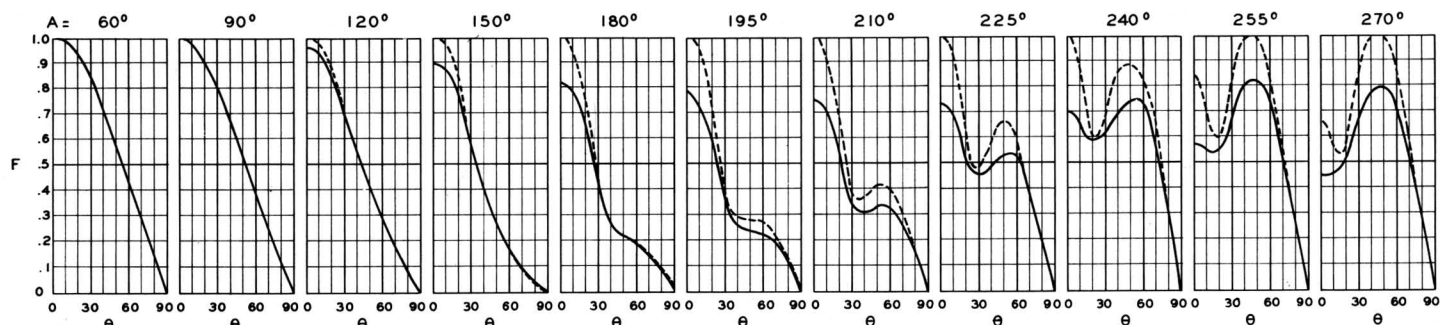


Fig. 35 – Measured field patterns of a triangular dipole for various dipole lengths and flare angle (α) = 40° . The patterns in the XZ plane are indicated by the solid curves, and the patterns in the XY plane by the dashed curves.

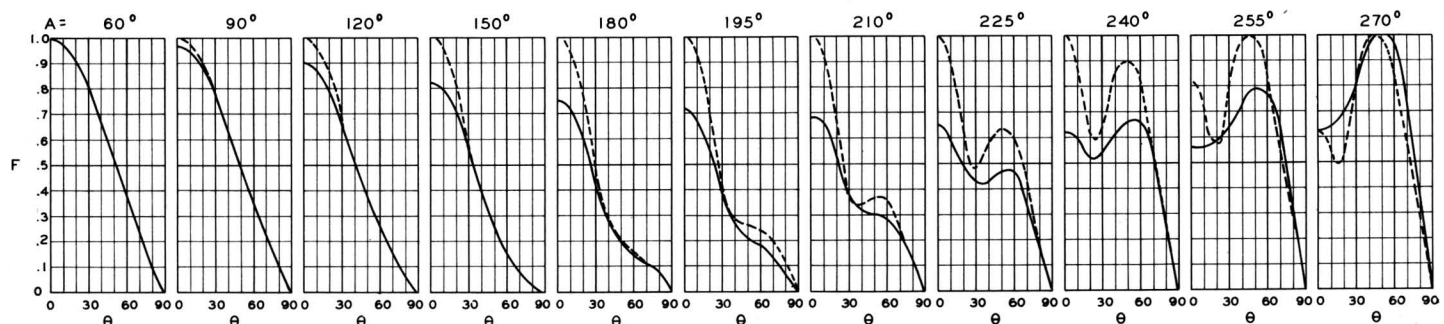


Fig. 36 – Measured field patterns of a triangular dipole for various dipole lengths and flare angle (α) = 50° . The patterns in the XZ plane are indicated by the solid curves, and the patterns in the XY plane by the dashed curves.

Experimentally Determined Radiation Characteristics of Conical and Triangular Antennas

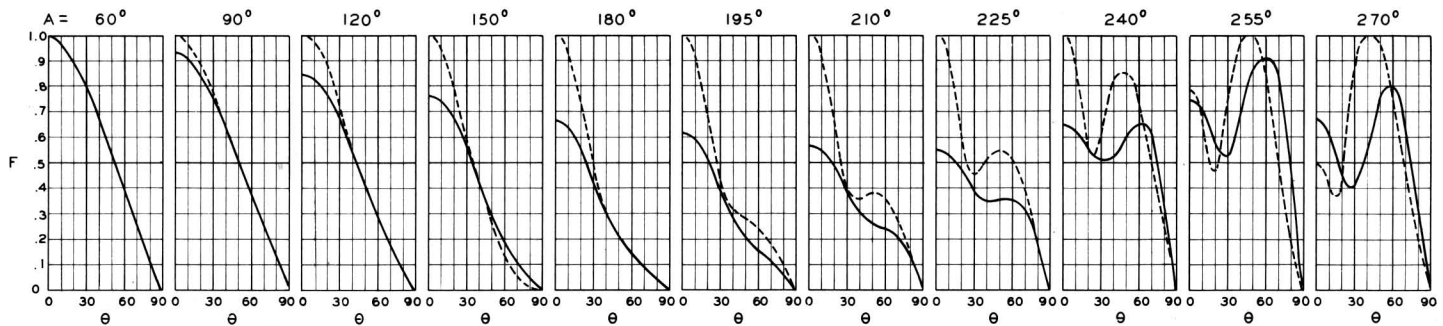


Fig. 37 – Measured field patterns of a triangular dipole for various dipole lengths and flare angle (α) = 60° . The patterns in the XZ plane are indicated by the solid curves, and the patterns in the XY plane by the dashed curves.

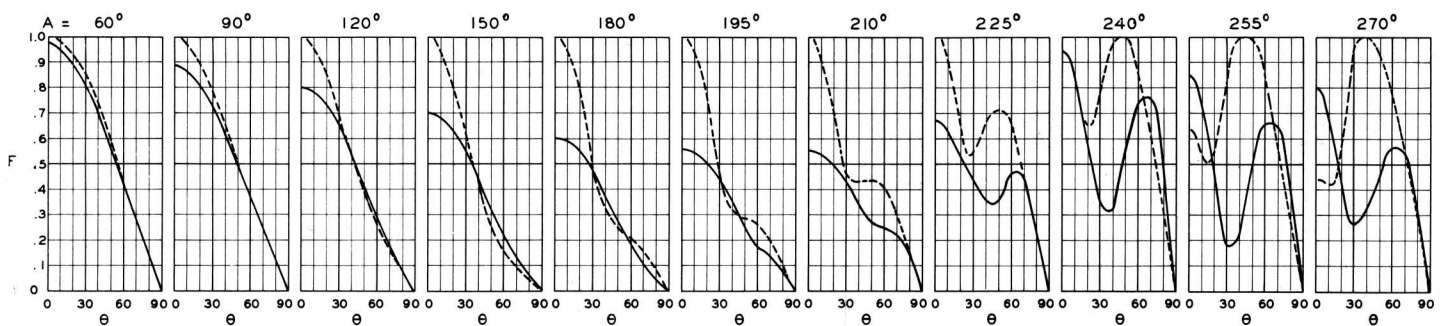


Fig. 38 – Measured field patterns of a triangular dipole for various dipole lengths and flare angle (α) = 70° . The patterns in the XZ plane are indicated by the solid curves, and the patterns in the XY plane by the dashed curves.

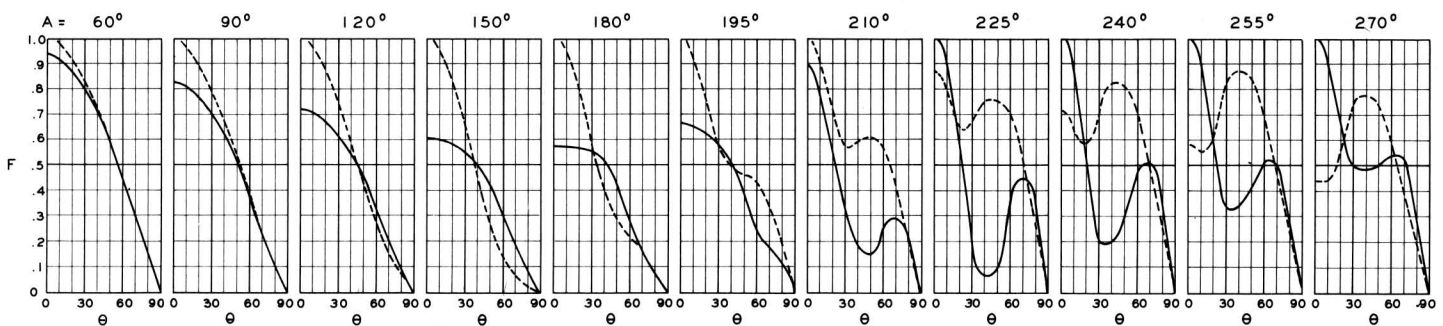


Fig. 39 – Measured field patterns of a triangular dipole for various dipole lengths and flare angle (α) = 80° . The patterns in the XZ plane are indicated by the solid curves, and the patterns in the XY plane by the dashed curves.

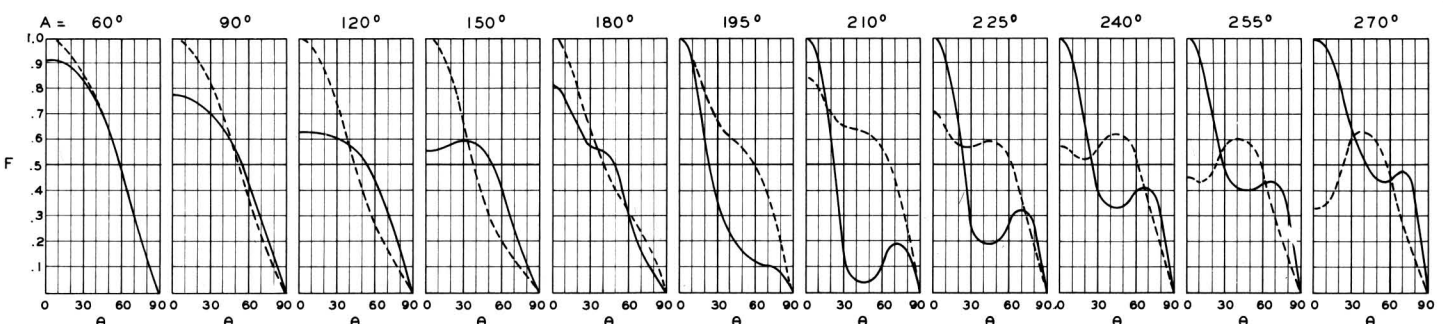


Fig. 40 – Measured field patterns of a triangular dipole for various dipole lengths and flare angle (α) = 90° . The patterns in the XZ plane are indicated by the solid curves, and the patterns in the XY plane by the dashed curves.

Triangular Antenna Field Pattern Measurements

The measured relative field patterns for the triangular dipoles are plotted in Figs. 31 to 40 in the same manner as for the conical dipoles. Patterns taken in the XY plane are shown as dashed curves and patterns taken in the XZ plane as solid curves.

The two patterns depart considerably for triangular dipoles of large flare angle and long length.

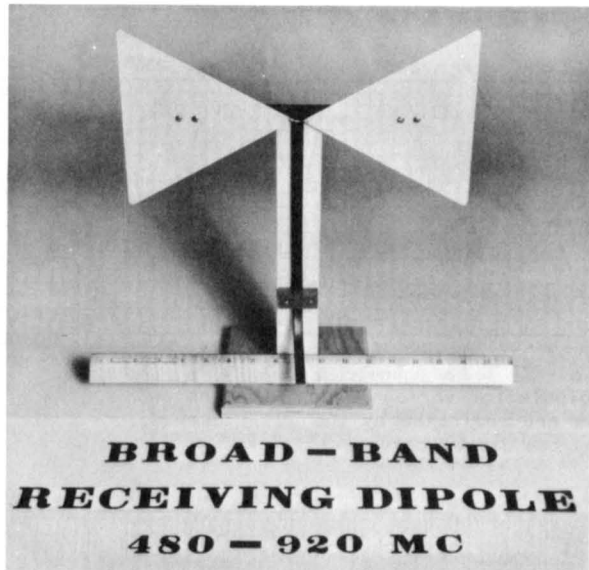


Fig. 41 - An application of the measured impedance data to a practical receiving dipole.

As the triangle field patterns do not always have circular symmetry in one plane, the power gain measurement described previously could not be used. No other method of determining the power gain was attempted.

Fig. 41 shows an application of the measured data to a particular design example. A

FAN DIPOLE

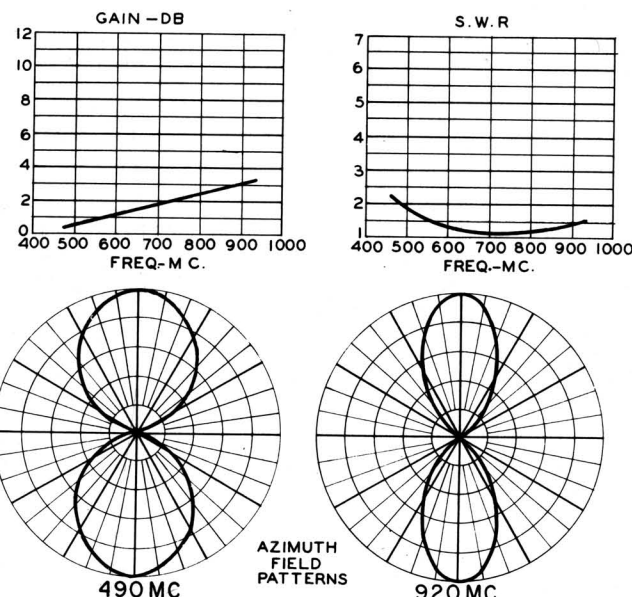
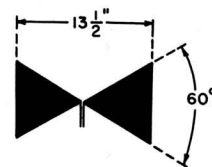


Fig. 42 - Measured characteristics of fan dipole.

broad-band dipole was required¹² for receiving use with 300-ohm characteristic-impedance line in the UHF range of 480 Mc to 920 Mc.

The dipole was made in the form of triangular elements supported by an insulating arm. From a study of the impedance data of Figs. 27 and 28, a flare angle of 60 degrees and total length of $13\frac{1}{2}$ inches was chosen as a suitable compromise to limit the standing-wave ratio to 2:1 or less over the frequency range. The final measured results are shown in Fig. 42.

O. M. Woodward Jr.

O. M. Woodward, Jr.

George H. Brown

George H. Brown

References

¹Nils E. Lindenblad, "Television Transmitting Antenna for Empire State Building", *RCA Review*, Vol. 3, No. 4, p. 387, (April, 1939).

²P. D. Smith, "The Conical Dipole of Wide Angle", *Journal of Applied Physics*, Vol. 19, No. 1, p. 11, (January, 1948).

³C. T. Tai, "On the Theory of Biconical Antennas", *Journal of Applied Physics*, Vol. 19, No. 12, p. 1155, (December, 1948).

⁴P. D. P. Smith, "Comments on Biconical Antennas", *Journal of Applied Physics*, Vol. 20, No. 6, p. 633, (June, 1949).

⁵C. T. Tai, "A study of the e.m.f. Method", *Journal of Applied Physics*, Vol. 20, No. 7, p. 717, (July, 1949).

⁶Charles H. Papas and Ronald King, "Input Impedance of Wide-Angle Conical Antennas Fed by a Coaxial Line", *Proc. I.R.E.*, Vol. 37, No. 11, p. 1269, (November, 1949).

⁷Charles H. Papas and Ronald King, "Radiation from Wide-Angle Conical Antennas Fed by a Coaxial Line", *Proc. I.R.E.*, Vol. 39, No. 1, p. 49, (January, 1951).

⁸S. A. Schelkunoff, "General Theory of Symmetric Biconical Antennas", *Journal of Applied Physics*, Vol. 22, No. 11, pp. 1330-1332, (November, 1951).

⁹L. Essen and M. H. Oliver, "Aerial Impedance Measurements", *Wireless Engineer*, Vol. 22, No. 267, p. 587, (December, 1945).

¹⁰George H. Brown and O. M. Woodward, Jr., "Experimentally Determined Impedance Characteristics of Cylindrical Antennas", *Proc. I.R.E.*, Vol. 33, No. 4, p. 257, (April, 1945).

¹¹J. F. Morrison and P. H. Smith, "The Shunt-Excited Antenna", *Proc. I.R.E.*, Vol. 25, No. 6, p. 690, (June, 1937).

¹²George H. Brown, "Field Test of Ultra-High-Frequency Television in the Washington Area", *RCA Review*, Vol. 9, No. 4, p. 572, (December, 1948).